# Flow Characteristics of Three Enhanced Oil Recovery Polymers in Porous Media

**Bing Wei**

Department of Chemical Engineering, University of New Brunswick, Fredericton E3B 5A3, Canada
Correspondence to: B. Wei (E-mail: bing.wei@unb.ca)

**ABSTRACT:** This article presents an experimental study aiming to explore the relationship among rheological properties, flow characteristics in porous media, and enhanced oil recovery (EOR) performance of three typical EOR polymers. The results suggest that xanthan gum exhibits a very pronounced shear-thinning behavior, which is probably also the reason explaining its moderate adsorption extent within porous media (thickness of adsorbed layer, $e = 3.1$ $\mu$m). The advanced viscoelastic properties coupled with the less adsorption extent compared to the hydrophobically modified copolymer (HMSPAM) allow xanthan gum to establish a "piston-like" displacement pattern and lead up to 49.4% original oil in place (OOIP) of the cumulative oil recovery during polymer flooding. Regarding HMSPAM, the significant permeability reduction of the porous media induced by multilayer adsorption ($e = 5.6$ $\mu$m) results in much higher drive forces ($\Delta P$) in the extended waterflooding stage, which further raises the cumulative oil recovery by 18.5% OOIP. In general, xanthan gum and HMSPAM totally produced 84% OOIP which is 15% higher than the extensively used EOR polymer, hydrolyzed polyacrylamide (HPAM), under the same experimental conditions. © 2014 Wiley Periodicals, Inc. J. Appl. Polym. Sci. **2015**, *132*, 41598.

## INTRODUCTION

For most of the oilfields in the world, at least half of the reserved oil still leaves behind after the primary (natural flow or artificial lift) and secondary recovery (waterflooding) methods are exhausted.[1] Numerous techniques have been established in the past decades aiming to enhance the oil recovery of the viscous fingered/channelled reservoirs after extensive water injection.[2–5] This process is so-called tertiary or enhanced oil recovery (EOR). Among all the EOR techniques, polymer flooding is one of the most promising techniques because of the relatively lower capital cost.[6–8]

Polymer flooding refers to the thickening of the displacing water with a small quantity of water-soluble polymer. It has been recognized that to achieve a stable displacement front, the mobility ratio defined as the mobility of displacing phase (i.e. water) relative to that of displaced phase (i.e. oil) must be equal to or less than 1. However, in reality, the low viscosity of water compared to crude oil usually leads to a much higher value and thus results in a very limited oil recovery. Using polymers can improve the mobility ratio through increasing the viscosity of water and reducing the permeability of porous media. The oil recovery mechanisms of polymer flooding have been intensively reviewed in our previous report.[9] Broadly speaking, polymer flooding is capable of raising the sweep efficiency owing to the viscous property; meanwhile, it also can improve the displacement efficiency by mobilizing the capillary force trapped residual oil as a result of the elastic property.

Partially hydrolyzed polyacrylamide (HPAM) is the most widely used polymer to date in polymer flooding EOR because of their availability in large quantity with customized properties (molecular weight, hydrolysis degree, etc.) and low manufacturing cost.[10,11] However, this kind of polymer is susceptible to harsh reservoir conditions such as elevated temperature, salinity, and shear forces, which significantly affects their performance in EOR.[12–16] Another type of polymer which is also being used in oilfields is biopolymer, i.e. xanthan gum, which is a biologically produced polysaccharide. This polymer is believed to be an alternative to HPAM due to the great tolerance to mechanical shear, temperature, and salinity.[17–20] Moreover, a series of hydrophobically modified copolymers, incorporating a small fraction of hydrophobic monomers into the backbone of polyacrylamide, have been recently proposed in the market.[21–23] The hydrophobic interactions in aqueous solution can enlarge the hydrodynamic size of polymer chains and in turn render the polymer solution superior viscosity and other related features.[24] This favorable property makes hydrophobically modified

**Table I.** Properties of the Evaluated Polymer Systems

| Name | Molecular weight ($10^6$ g/mol) | Hydrolysis (%) | Concentration (wt %) | Shear viscosity @ 6 s$^{-1}$ (mPa·s) | Supplier |
|---|---|---|---|---|---|
| HPAM | 8 | 5 | 1.0 | 466 | Gel Technologies, USA |
| Xanthan gum | 2–5 | – | 0.4 | 485 | El Peto Products, Canada |
| HMSPAM | 6 | – | 0.7 | 478 | BSAF, Germany (Proprietary) |

copolymers promising flooding agents in EOR process in the near future.

It has been proved that the flow behavior of EOR polymers in porous media is closely associated with their solution properties.[25,26] Visual study performed by Buchgraber et al.[27] and Aktas et al.[28] observed that polymer flooding (HPAM) is able to mitigate viscous fingers and improve the sweep efficiency in different extent depending on solution viscosity. In addition to viscosity, elasticity also plays an important role in maintaining the stability of the displacement front.[29] Therefore, this work selected three typical EOR polymers including a partially hydrolyzed polyacrylamide (HPAM), a xanthan gum, and a hydrophobically modified copolymer (HMSPAM), and investigated their rheological properties, flow characteristics, and enhanced oil recovery performance. The primary objective of this article was to relate the bulk properties of polymer solutions to their flow behavior in porous media. To accompany this objective, rheological analysis was initially performed followed by core flood tests conducted in glass-bead packs. Finally, the propagation pattern during polymer displacing residual oil in porous media was proposed based on oil recovery performance.

## EXPERIMENTAL

### Materials
Three different types of EOR polymers were used in this study and their basic properties are given in Table I. The proprietary hydrophobic polymer (HMSPAM) is an acrylamide-based copolymer which contains a small fraction of hydrophobic pendant groups.[21,30] The synthetic brine was prepared with the inorganic salt of NaCl, MgCl$_2$, CaCl$_2$, and Na$_2$SO$_4$ in laboratory. The ionic concentrations of the salt are listed in Table II. The total salinity is the sum of the ionic concentrations. The crude oil sample (approximately 1000 mPa·s at 25°C) was kindly provided by Husky Energy, Alberta, Canada.

### Rheological Analysis
Polymer solutions having shear viscosity around 470 mPa·s at 6 s$^{-1}$ were prepared by dissolving polymer powders in the synthetic brine (Table II) and then shaken for 1–2 days using a KS 130 basic shaker (IKA®, Canada) to ensure complete dissolution.

**Table II.** Composition of the Synthetic Brine

| Total salinity (ppm) | $C_{cation}$ (ppm) | | | $C_{anion}$ (ppm) | |
|---|---|---|---|---|---|
| | Na$^+$ | Mg$^{2+}$ | Ca$^{2+}$ | Cl$^-$ | SO$_4{}^{2-}$ |
| 46,970 | 17,380 | 900 | 3200 | 25,400 | 90 |

Viscometric measurements were carried out on a Bohlin Gemini HR Nano Rheometer equipped with a cone and plate geometry (2°/55 mm) at 25°C. Dynamical shear measurements were performed with the rheometer equipped with a parallel geometry (60 mm) and 1 mm gap size at 25°C to determine the elastic ($G'$) and viscous ($G''$) moduli of the polymer systems as a function of angular frequency ranging from 0.01 to 100 rad/s. It should be noted that all dynamical measurements were preceded by an oscillation strain sweep to identify the linear viscoelastic region of the polymers. All the measurements were performed in the linear response region of the samples.
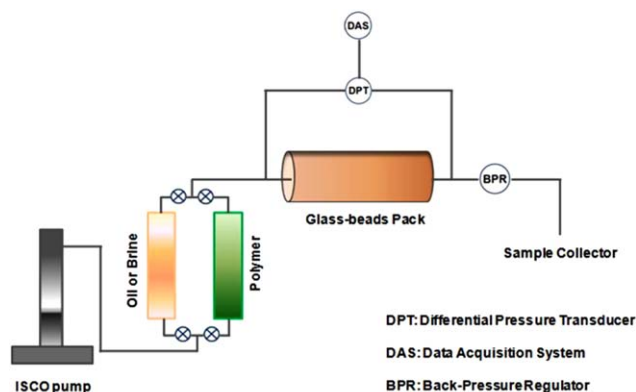
### Core Flood Tests
**Preparation of Glass-Bead Packs.** The porous media used in this work is granular pack composed of glass beads with an average size ranging from 80 to 200 $\mu$m. The glass beads were vertically packed for 3–4 days in a rubber sleeve and then assembled in core flood rig as illustrated in Figure 1.

Distilled water was then injected into the dried glass-bead packs to measure the pore volume (PV) followe by several PVs of brine injection. The average permeability to brine could be calculated using Darcy's Law [eq. (1)].[31]

$$k_{brine} = \frac{L}{A} \cdot \mu \cdot Q \cdot \frac{1}{\Delta P} \qquad (1)$$

where $k_{brine}$ is the brine permeability (D), $L$ is the length of the pack (cm), $A$ is the cross-sectional area of the pack, $\mu$ is the viscosity of the fluid (mPa·s), $Q$ is the flow rate (cm$^3$/s), and $\Delta P$ is the differential pressure across the pack (atm).

In addition, the effective shear rate in the porous media was estimated by the following equation [eq. (2)].[29,32]



**Figure 1.** Layout of the core flood test set-up. [Color figure can be viewed in the online issue, which is available at wileyonlinelibrary.com.]

**Table III.** Properties of the Glass-Bead Packs

| Property | HPAM | Xanthan gum | HMSPAM |
|---|---|---|---|
| Permeability, $k_{brine}$ (D) | 4.49 | 3.98 | 3.01 |
| Length, $L$ (cm) | 15.0 | 15.0 | 15.0 |
| Cross-sectional area, $A$ (cm$^2$) | 47.76 | 47.76 | 47.76 |
| Porosity, $\varphi$ (%) | 39.6 | 39.2 | 39.8 |
| Shear rate, $\gamma$ s$^{-1}$) | 5.0 | 5.2 | 6.0 |
| Pore volume, PV (mL) | 278.3 | 266.8 | 270.0 |
| System pressure (psi) | 550.0 | 550.0 | 550.0 |
| Initial oil saturation, $S_{o,i}$ (% OOIP) | 98.2 | 96.6 | 98.6 |

$$\gamma = \frac{3n+1}{4n} \cdot \frac{4Q}{A(8k\varphi)^{1/2}} \quad (2)$$

where $\gamma$ is the shear rate (s$^{-1}$), $(3n+1)/4n$ is a non-Newtonian correction factor for power-law fluids, $Q$ is flow rate (cm$^3$/s), $A$ is the cross-sectional area of the pack (cm$^2$), $k$ is the permeability (cm$^2$), and $\varphi$ is the porosity. For the fluids used in this study, $n$ values changed between 0.45 and 0.56.

Table III lists the physical properties of the prepared glass-bead packs.

**Injection of Polymer Solutions.** The flow behavior of the polymer systems was evaluated by injecting the corresponding polymer solutions through the glass-bead packs until the differential pressure between the inlet and outlet ($\Delta P$) leveled off. Afterwards, brine injection was resumed until $\Delta P$ values held constant. Herein, two factors including resistant factor (RF) and residual resistant factor (RRF) which are closely related to the applicability of polymers in enhanced oil recovery were determined. The resistant factor provides the effective viscosity or mobility control ability of polymers during traveling in porous media, while the residual resistant factor measures the permeability reduction of porous media caused by polymer
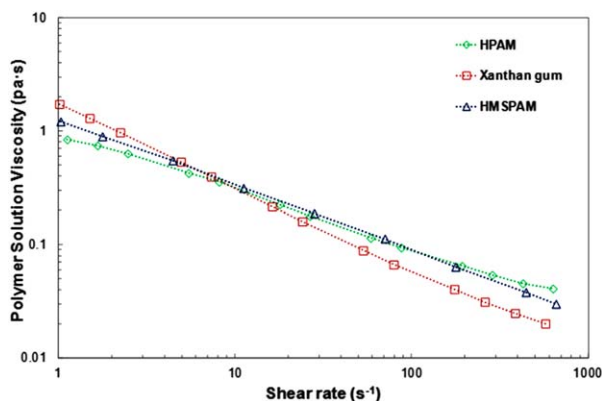


**Figure 2.** Stead shear viscosity of polymer solutions versus shear rate. [Color figure can be viewed in the online issue, which is available at wileyonlinelibrary.com.]
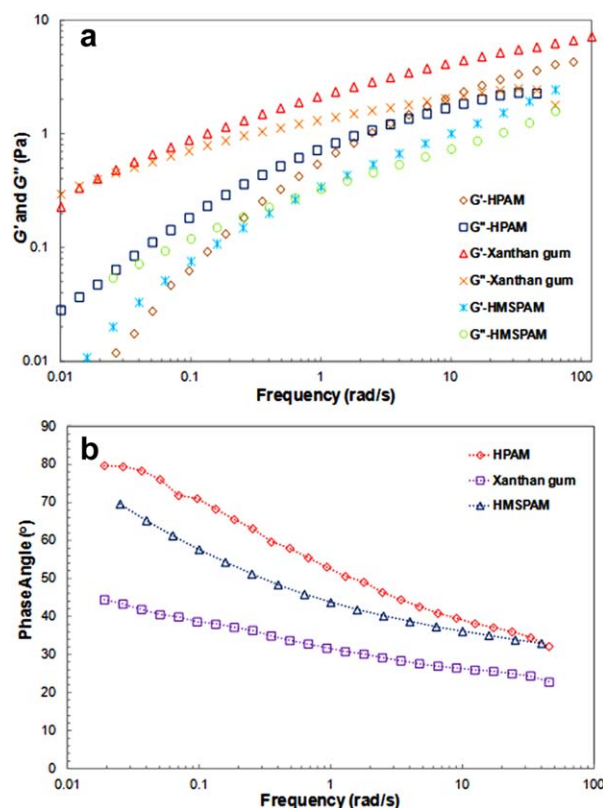


**Figure 3.** (a) Elastic ($G'$) and viscous ($G''$) moduli and (b) phase angle versus frequency. [Color figure can be viewed in the online issue, which is available at wileyonlinelibrary.com.]

adsorption. The expressions of RF and RRF are given in eqs. (3) and (4).

$$RF = \frac{\Delta P_{Polymer}}{\Delta P_{Brine}} \quad (3)$$

$$RRF = \frac{\Delta P_{Brine\ after\ polymer\ injection}}{\Delta P_{Brine\ before\ polymer\ injection}} \quad (4)$$

The retained polymer within porous media was cleaned by flushing a bleaching solution to regain the original permeability. The glass-bead packs were then flooded with numerous PVs of distilled water and brine to remove any remaining bleach in porous media.

**Enhanced Oil Recovery.** The brine saturated glass-bead packs were flooded with the crude oil until the water fraction at the production end was zero. At this stage, the connate water saturation and oil saturation were determined based on the mass balance as presented in Table III. After that, brine was injected as the secondary oil recovery mode (waterflooding) followed by 1 PV (slug size) of polymer flooding and an extended waterflooding. All the fluids were injected at a low linear velocity of 1 foot per day.

## RESULTS AND DISCUSSION

### Rheological Properties

Figure 2 plots the shear viscosity of the polymer solutions as a function of shear rate. To describe the variation in the

**Table IV.** Rheological Properties of the EOR Polymers

| Polymer | Apparent viscosity | | | $G'$ | | | $G''$ | | |
|---|---|---|---|---|---|---|---|---|---|
| | $n$ | $k$ | $R^2$ | $n'$ | $k'$ | $R^2$ | $n''$ | $k''$ | $R^2$ |
| HPAM | 0.50 | 0.95 | 0.99 | 0.71 | 0.37 | 0.95 | 0.53 | 0.54 | 0.96 |
| Xanthan gum | 0.28 | 1.66 | 0.99 | 0.34 | 1.82 | 0.97 | 0.23 | 1.16 | 0.94 |
| HMSPAM | 0.42 | 1.25 | 0.99 | 0.61 | 0.26 | 0.97 | 0.30 | 0.41 | 0.99 |

rheological properties of the samples under steady shear, the experimental data were fitted to the well-known power-law model [eq. (5)], which is extensively used to study non-Newtonian fluids in theoretical analysis.[33]

$$\mu = K \ \dot{\gamma}^{n-1} \tag{5}$$

where, $\mu$ is the shear viscosity (mPa·s), $K$ is the consistency index, $\dot{\gamma}$ is the shear rate (s$^{-1}$), and $n$ is the flow behavior index.

It is clear that all three polymer solutions are pseudoplastic fluids which can be well described by the power-law model with very high determination coefficients ($R^2 = 0.99$). Apparently, xanthan gum exhibits the most pronounced shear-thinning behavior with the flow behavior index $n = 0.28$ in comparison with HPAM and HMSPAM.

Plots of elastic ($G'$) and viscous ($G''$) moduli of the polymers versus angular frequency [Figure 3(a)] indicate that the magnitudes of $G'$ and $G''$ increase with frequency. It is also noticed that xanthan gum possesses the greatest viscoelasticity relative to HPAM and HMSPAM particularly at low frequency. Table IV presents the slopes ($n'$ and $n''$), intercepts ($K'$ and $K''$), and $R^2$ of the rheological data described by the following equations [eqs. (6) and (7)].[34]

$$G' = K' \omega^{n'} \tag{6}$$

$$G'' = K'' \omega^{n''} \tag{7}$$

It can be seen that the slopes of xanthan gum with 0.34 ($G'$) and 0.23 ($G''$) are much lower than that of another two polymers, suggesting the slight dependency of the viscoelasticity on frequency. In other words, the $G'$ and $G''$ of HPAM and HMSPAM are closely related to the imposed angular frequency, and high frequency leads to high viscoelasticity. Figure 3(b) shows the phase angle variation as a function of frequency. It is found that the phase angle of xanthan gum is in the range of 25–45°, indicating the dominance of the elasticity compared to the viscosity. However, for HPAM and HMSPAM, it seems that the viscoelastic characteristics are highly dependent on the impose frequency, the viscous nature prevails over the elastic nature (phase angle ≥ 45°) below the frequency of 2 rad/s; however, when the frequency is above 2 rad/s, the elastic nature becomes more evident (phase angle < 45°).

These rheological observations can be generally attributed to the conformational status of polymer systems. For example, the molecules of xanthan gum tend to orderly associate through the weak hydrogen bonding and chain entanglement, which therefore results in a high viscosity at low shear rate; however, when

it is subjected to fast shear flow (high shear rate), the formed associations would be broken up leading to a remarkable decrease in solution viscosity.[35,36] The structured and gel-like associations render xanthan gum more elastic characteristic compared to viscous characteristic. Similar results were also observed for HMSPAM, whose viscosifying power is not only determined by the entanglements of polymer chains but also by the hydrophobic interactions. Nevertheless, there is a noticeable difference between xanthan gum and HMSPAM, namely flexibility of polymer chain. It has been well documented that due to the rigid of polysaccharide chains, xanthan gum is extremely tolerant to mechanical shear and salinity.[37] This maybe the reason that the viscoelastic properties of xanthan gum are slightly influenced by angular frequency as indicated by the low slopes ($n'$ and $n''$) (Table IV); on the contrary, the viscoelasticity of polyacrylamide and derivates is strongly affected by angular frequency as shown in Figure 3, the magnitudes of $G'$ and $G''$ increase more steeply than that of xanthan gum resulting from the stretching of polymer chains under the dynamical shear field.

**Flow in Porous Media**

Figure 4 plots the RF and RRF values developed during fluids injection. The RF values of all three polymer solutions show a similar trend, i.e., *RF* increases gently with the volume of injected polymer solutions and then reaches a steady stage after approximately 2 PVs. Apparently, the hydrophobically modified copolymer, HMSPAM, produced the highest *RF* values followed by xanthan gum and HPAM. In terms of *RRF*, as shown in Figure 4, after flushing several PVs of brine, they tended to be constant at different levels. Subsequently, the average thickness
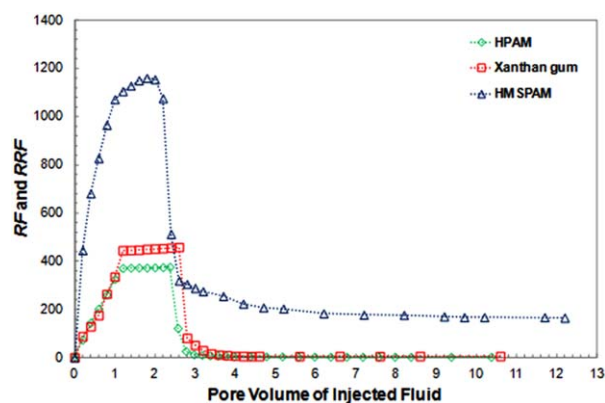


**Figure 4.** Resistant factor and residual resistant factor versus pore volume of injected fluids. [Color figure can be viewed in the online issue, which is available at wileyonlinelibrary.com.]

**Table V.** Summary of Fluids Injection Experiments

| Polymer | Pore volume of Injected Polymer solution (PV) | $RF^a$ | Pore volume of injected brine (PV) | $RRF^a$ | $r$ (μm) | $e$ (μm) | Quantity of adsorption (μg/ g glass bead) |
|---|---|---|---|---|---|---|---|
| HPAM | 2.3 | 376 | 8 | 2.6 | 9.5 | 2.0 | 405.7 |
| Xanthan gum | 2.6 | 446 | 8 | 5.7 | 9.0 | 3.1 | 465.4 |
| HMSPAM | 2.2 | 1127 | 10 | 165.2 | 7.8 | 5.6 | 801.7 |

$^a$ Represents the RF or RRF values when they hold constant.

of the hydrodynamic polymer layer was determined using eq. (8).[38–41]

$$e = r \cdot \left(1 - RRF^{-\frac{1}{4}}\right) \qquad (8)$$

where, $e$ is the average hydrodynamic polymer layer thickness (μm), $r$ is the average pore radius (μm) for brine flow which can be calculated using eq. (9),[38] and RRF is the residual resistant factor at the steady stage.

$$r = \left(\frac{8 \cdot k_{brine}}{\varphi}\right)^{1/2} \qquad (9)$$

where $k_{brine}$ is the brine permeability (D), and $\varphi$ is the porosity (fraction).

Table V lists the thickness of the adsorbed polymer layer on the surface of glass beads and the quantity of polymer adsorption measured by UV absorbance method.[42] It can be seen that HMSPAM produced the most significant $RRF$ corresponding to the thickness of the adsorbed polymer layer of 5.6 μm. This result could be interpreted by a mechanism called "multilayer adsorption" induced by the hydrophobic interactions.[43,44] Unlike HMSPAM, the built adsorbed layer of xanthan gum might be sheared off by the brine flow due to the relatively weaker hydrogen bonding forces, which in turn reduces the extent of adsorption. This result is somehow consistent with the rheological properties of the xanthan gum solution. The lowest thickness of the adsorbed layer is given by HPAM, which probably results from the negative charges providing repulsion between polymers and the surface of glass beads.[45]
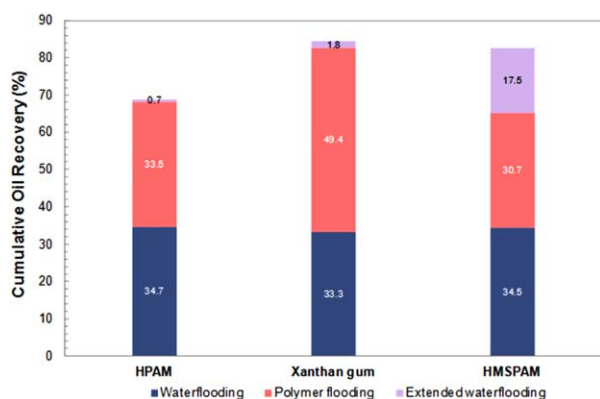
**Enhanced Oil Recovery**

The functionality of polymer systems in displacing crude oil in place was investigated by simulating oilfield production process. In this study, it was found that after 8 PVs of brine injection, the produced Water/Oil Ratio (WOR) at the end of the packs was nearly zero, indicating that the waterflooding method has been exhausted. Hence, a polymer slug with the size of 1 PV was injected as the enhanced oil recovery mode followed by an extended waterflooding until the WOR was zero again. Figure 5 displays the percentage of the cumulative oil recovery achieved in each stage.

The oil recovery results show that xanthan gum and HMSPAM totally recovered around 15% OOIP more oil than HPAM under the identical experimental conditions due to their high mobility control capacities. The mobility control or mobility reduction of polymer systems represented by RF can be generally ascribed to three mechanisms: (1) viscosity, (2) elasticity,[26] and (3) permeability reduction (or RRF). It is believed that at the similar viscosity, the mobility control capacity of HMSPAM is governed by the permeability reduction caused by the significant polymer adsorption. However, for xanthan gum, this capacity is more likely governed by the viscoelastic properties owing to the low adsorption extent and high mechanical stability, which accordingly maintains a stable displacing or propagating front. This makes xanthan gum enhance both of the sweep efficiency and the displacement efficiency during flooding the residual oil saturated porous media. This fact can also be understood in the oil recovery performance as shown in Figure 5. As seen, 49.4% OOIP was recovered by 1 PV of xanthan gum,
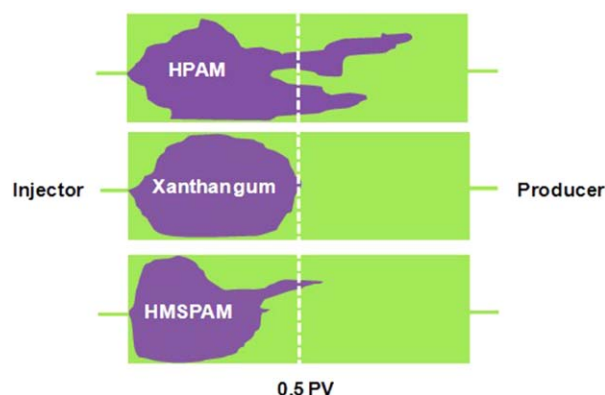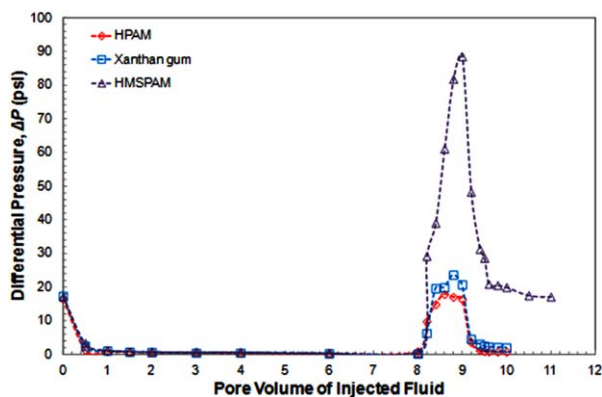


**Figure 5.** Cumulative oil recovery by waterflooding, polymer flooding, and extended waterflooding. [Color figure can be viewed in the online issue, which is available at wileyonlinelibrary.com.]



**Figure 6.** Schematic representation of the displacement pattern of polymers in porous media at 0.5 PV. [Color figure can be viewed in the online issue, which is available at wileyonlinelibrary.com.]

**Figure 7.** Differential pressure developed during waterflooding, polymer flooding and extended waterflooding.0–8 PVs: waterflooding; 8–9 PV: polymer flooding; 9–12 PVs: extended waterflooding. [Color figure can be viewed in the online issue, which is available at wileyonlinelibrary.com.]

which is 18% OOIP higher than HMSPAM flooding. It is implied that xanthan gum exhibits a "piston-like" displacement pattern in the porous media, while HPAM and HMSPAM developed some viscous fingers in the propagating front as depicted in Figure 6. This result is consistent with previous reports.[27,29]

In the stage of the extended waterflooding, it is found that HMSPAM recovered up to 17.5% OOIP and xanthan gum recovered only 1.8% OOIP, this can be interpreted as that the significant permeability reduction of the porous media requires a high pressure drop ($\Delta P$) to drive the brine flowing through the packs as indicated in Figure 7, which correspondingly further improved the sweep efficiency and/or displacement efficiency of the HMSPAM flooding. Nevertheless, in the case of xanthan gum and HPAM, the chase brine can easily channel through the porous media without any distinct increase in the cumulative oil recovery as shown in Figure 5.

## CONCLUSIONS

The rheological properties, flow characteristics, and enhanced oil recovery performance of three typical EOR polymers were investigated in this work attempting to relate the bulk solution properties to the flow behavior in porous media. The main conclusions drawn from this study are as follows:

1. Xanthan gum exhibits the most pronounced shear-thinning property compared to HMSPAM and HPAM, which leads to a moderate adsorption extent within porous media.
2. The hydrophobically modified copolymer, HMSPAM, produced the highest RF and RRF because of the significant polymer adsorption induced by the hydrophobic interactions. The average thickness of the adsorbed HMSPAM layer is 5.6 $\mu$m, which is much higher than that of xanthan gum (3.1 $\mu$m) and HPAM (2.0 $\mu$m).
3. Under the same experimental conditions, HMSPAM and xanthan gum can recover 15% OOIP more oil than HPAM resulting from the considerable mobility reduction. Xanthan gum exhibits a "piston-like" displacement front which can produce more oil during polymer flooding than HMSPAM and HPAM. But a higher cumulative oil recovery was

obtained for HMSPAM during the extended waterflooding due to the high differential pressure ($\Delta P$) induced by the remarked permeability reduction.

## REFERENCES

1. Thomas, S. *Oil Gas Sci. Technol.* **2008**, *63*, 9.
2. Shiran, B. S.; Skauge, A. *Energy Fuels* **2013**, *27*, 1223.
3. Jiang, Q.; Thornton, B.; Russel-Houston, J.; Spence, S. *J. Can. Pet. Technol.* **2010**, *49*, 57.
4. Sun, J.; Li, Z.; Wu, G. *IPTC 14582*, **2011**.
5. Jeirani, Z.; Mohamed Jan, B.; Si Ali, B.; Noor, I. M.; See, C. H.; Saphanuchart, W. *J. Ind. Eng. Chem.* **2013**, *19*, 1310.
6. Algharaib, M.; Alajmi, A.; Gharbi, R. *J. Petrol. Sci. Eng.* **2014**, *115*, 17.
7. Gonzalez Da Silva, I. P.; De Melo, M. A.; Luvizotto, J. M.; Lucas, E. F. *SPE 107727*, **2007**, *2*, 999.
8. Wang, J.; Liu, H. *J. Ind. Eng. Chem.* **2014**, *20*, 656.
9. Wei, B.; Romero-Zerón, L.; Rodrigue, D. *J. Pet. Explor. Prod. Technol.* **2013**, *4*, 113.
10. Needham, R. B.; Doe, P. H. *J. Petrol. Technol.* **1987**, *39*, 1503.
11. Dong, H. Z.; Fang, S. F.; Wang, D. M.; Wang, J. Y.; Liu, Z.; Hong, W. H. *SPE 114342*, **2008**, *3*, 1520.
12. Muller, G. *Polym. Bull.* **1981**, *5*, 31.
13. Al Hashmi, A. R.; Al Maamari, R. S.; Al Shabibi, I. S.; Mansoor, A. M.; Zaitoun, A.; Al Sharji, H. H. *J. Pet. Sci. Eng.* **2013**, *105*, 100.
14. Seright, R. S. *SPE J.* **1983**, *23*, 475.
15. Rashidi, M.; Blokhus, A. M.; Skauge, A. *J. Appl. Polym. Sci.* **2010**, *117*, 1551.
16. Samanta, A.; Bera, A.; Ojha, K.; Mandal, A. *J. Chem. Eng. Data* **2010**, *55*, 4315.
17. Guo, X. H.; Li, W. D.; Tian, J.; Liu, Y. Z. *SPE 57294*, **1999**.
18. Kohler, N.; Chauveteau, G. *J. Petrol. Technol.* **1981**, *33*, 349.
19. Wei, B.; Romero-Zerón, L.; Rodrigue, D. *Polym. Eng. Sci.* **2014**. DOI: 10.1002/pen.239.
20. Jang, H. Y.; Zhang, K.; Chon, B. H.; Choi, H. J. *J. Ind. Eng. Chem.* **2014**.
21. Reichenbach-Klinke, R.; Langlotz, B.; Wenzke, B.; Spindler, C.; Brodt, G. *SPE 141107*, **2011**, *1*, 356.
22. Taylor, K. C.; Nasr-El-Din, H. A. *J. Petrol. Sci. Eng.* **1998**, *19*, 265.

23. Zaitoun, A.; Makakou, P.; Blin, N.; Al-Maamari, R. S.; Al-Hashmi, A. R.; Abdel-Goad, M.; Al-Sharji, H. H. *SPE J.* **2012**, *17*, 335.

24. Lai, N.; Dong, W.; Ye, Z.; Dong, J.; Qin, X.; Chen, W.; Chen, K. *J. Appl. Polym. Sci.* **2013**, *129*, 1888.

25. Seright, R. S.; Fan, T.; Wavrik, K.; Wan, H.; Gaillard, N.; Favéro, C. *SPE Reserv. Eva. Eng.* **2011**, *14*, 726.

26. Urbissinova, T. S.; Trivedi, J. J.; Kuru, E. *J. Can. Pet. Technol.* **2010**, *49*, 49.

27. Buchgraber, M.; Clemens, T.; Castanier, L. M.; Kovscek, A. R. *SPE Reserv. Eva. Eng.* **2011**, *14*, 269.

28. Aktas, F.; Clemens, T.; Castanier, L. M.; Kovscek, A. R. *SPE* 113264, **2008**, *1*, 384.

29. Veerabhadrappa, S. K.; Trivedi, J. J.; Kuru, E. *Ind. Eng. Chem. Res.* **2013**, *52*, 6234.

30. Wei, B.; Romero-Zerón, L.; Rodrigue, D. *Polym. Adv. Technol.* **2014**, *25*, 732.

31. Takeuchi, S.; Nakashima, S.; Tomiya, A. *J. Volcanol. Geotherm. Res.* **2008**, *177*, 329.

32. Christopher, R. H.; Middleman, S. *Ind. Eng. Chem. Fundam.* **1965**, *4*, 422.

33. Sochi, T. *J. Polym. Sci, Part B: Polym. Phys.* **2010**, *48*, 2437.

34. Choi, H. M.; Yoo, B. *Food Chem.* **2009**, *116*, 638.

35. Moschakis, T.; Murray, B. S.; Dickinson, E. *J. Colloid Interface Sci.* **2005**, *284*, 714.

36. Song, K. W.; Kim, Y. S.; Chang, G. S. *Fibers Polym.* **2006**, *7*, 129.

37. Alquraishi, A. A.; Alsewailem, F. D. *Carbohydr. Polym.* **2012**, *88*, 859.

38. Zaitoun, A.; Kohler, N. *SPE* 18085, **1988**.

39. Wever, D. A. Z.; Picchioni, F.; Broekhuis, A. A. *Ind. Eng. Chem. Res.* **2013**, *52*, 16352.

40. Dupuis, G.; Rousseau, D.; Tabary, R.; Grassi, B. *SPE J.* **2011**, *16*, 43.

41. Denys, K.; Fichen, C.; Zaitoun, A. *SPE* 64984, **2001**.

42. Wei, B.; Romero-Zerón, L.; Rodrigue, D. *J. Macromol. Sci., Part B: Phys.* **2014**, *53*, 625.

43. Volpert, E.; Selb, J.; Candau, F.; Green, N.; Argillier, J. F.; Audibert, A. *Langmuir* **1998**, *14*, 1870.

44. Argillier, J. F.; Audibert, A.; Lecourtier, J.; Moan, M.; Rousseau, L. *Colloids Surf. A* **1996**, *113*, 247.

45. Lake, L. W. Enhanced Oil Recovery; Prentic Hall, New Jersey, **1989**.